

DENSE CORES OF DARK CLOUDS. XII. ^{13}CO AND C^{18}O IN LUPUS, CORONA AUSTRALIS, VELA, AND SCORPIUS

J. W. S. VILAS-BOAS

Centro de Aplicações Espaciais (CRAAE-INPE), Instituto Presbiteriano Mackenzie, R. Consolidação, 89, São Paulo, SP, Brazil CEP 01302-000, and Harvard-Smithsonian Center for Astrophysics

P. C. MYERS

Harvard-Smithsonian Center for Astrophysics, 60 Garden Street, Cambridge, MA 02138

AND

G. A. FULLER

National Radio Astronomy Observatory and Department of Physics, University of Manchester Institute of Science and Technology, P.O. Box 88, Manchester, M60 1QD, UK

Received 1998 October 6; accepted 1999 October 21

ABSTRACT

More than 110 dense condensations of the dark clouds in Lupus, Corona Australis, Norma, Vela, and Scorpius were observed in the ^{13}CO and C^{18}O ($J = 1-0$) transitions. The condensations of dark clouds with high star formation activity like the Ophiuchus, Taurus, and Cepheus have average C^{18}O and H_2 column densities of 1.8×10^{15} and $1.1 \times 10^{22} \text{ cm}^{-2}$. If we take the average size of the condensations to be 0.2 pc, a condensation must have average H_2 volumetric densities $\geq 2 \times 10^4 \text{ cm}^{-3}$ in order to be a good candidate to form stars. The four Lupus filaments have similar radial velocities and velocity dispersions, suggesting that they originated from the same parental cloud. Among these filaments, Lupus 1 is unique in having recent star formation activity, despite the high number of T Tauri stars observed toward the others. Lupus 1 also shows a complex velocity gradient along its main axis. The distribution of radial velocities of the condensations observed toward Scorpius are in good agreement with the hypothesis that they are in a region with expansion velocity smaller than or equal to 18 km s^{-1} . The Corona Australis cloud has velocity gradients ranging from $-0.5 \text{ km s}^{-1} \text{ pc}^{-1}$ at one extreme to $0.1 \text{ km s}^{-1} \text{ pc}^{-1}$ at the other.

Subject headings: ISM: clouds — ISM: molecules — stars: pre-main-sequence — submillimeter

1. INTRODUCTION

The millimeter wavelength rotational lines of carbon monoxide and its isotopic varieties have been widely used to probe dense condensations of nearby dark clouds. The observation of these lines has given important information about the condensations and their relation to star formation activity (Myers, Linke, & Benson 1983; Turner, Rickard, & Xu 1989). However, comparisons of the properties of the condensations in a complex, and from complex to complex, are still needed to understand the clouds and star formation.

Extensive surveys of dense condensations of the northern and southern hemisphere dark clouds Taurus, Ophiuchus, Cepheus, Vela, Musca, the Coalsack, and Chameleon II and III (Myers et al. 1983, hereafter MLB; Vilas-Boas, Myers, & Fuller 1994, hereafter VMF) have been done to compare the condensation properties observed in these clouds. Analyzing the mean properties of the condensation of these dark clouds, VMF showed that Chameleon III, which does not have any pre-main-sequence object associated with it, has significantly smaller column densities of dust and gas than Taurus and Ophiuchus. They also proposed that the condensations of Chameleon III are not “ready” to form stars as they have mean H_2 column densities much smaller than $7 \times 10^{21} \text{ cm}^{-2}$. Another remarkable result was the observed ^{13}CO ($J = 1-0$) line width, which is 2 times wider in Ophiuchus, which is an active site of star formation, than is observed toward other dark clouds, suggesting some relation between star formation and the mechanism producing the observed line widths.

Several other dark clouds were not included in these surveys, particularly the complexes of Lupus and Corona Australis, which are very important dark clouds in the southern hemisphere. The Lupus complex is known to host a large population of T Tauri stars, separated into four subgroups, with only one embedded *IRAS* source (B228). Corona Australis is a complex in which the main filament is a region of very recent and active star formation (Graham 1992) with several embedded infrared sources and variable stars.

In this paper we present an extended survey of the ^{13}CO and C^{18}O ($J = 1-0$) rotational transitions toward optically selected condensations in Lupus, Corona Australis, Vela, Norma, Scorpius, and one position in Carina. The selected positions are apparent maxima of visual extinction. The main purpose of this survey is to compare the properties of the condensations observed in these regions with those observed by MLB and VMF. The data accumulated from these surveys cover almost all known nearby dark clouds.

The source selection and the CO observations are described in §§ 2 and 3, and in §§ 4 and 5 the method of data reduction and analysis are presented. In §§ 6 and 7 the main properties of the molecular dark clouds and the individual regions are discussed, and finally in § 8 the paper is summarized. The data accumulated from this and the other surveys cover almost all known nearby dark clouds.

Our main results are (1) that the condensations observed in the Ophiuchus and Corona Australis main filaments, which are very active sites of star formation, have the highest average C^{18}O and H_2 column densities among the

TABLE 1A—Continued

CLOUD	CONDENSATION NAME	RA(1950)	decl.(1950)	$^{13}\text{CO} (J = 1-0)$				$^{18}\text{O} (J = 1-0)$				OPTICAL SIZE			COMMENTS
				T_A^* (K)	V_{LSR} (km s $^{-1}$)	ΔV (km s $^{-1}$)	T_A^* (K)	V_{LSR} (km s $^{-1}$)	ΔV (km s $^{-1}$)	l (arcmin)	b (arcmin)	A_V (mag)			
	Sc22	17 18 10	-44 05 54	6.81 ± 0.10	-12.80	2.08	1.07 ± 0.07	-12.79	1.75	5.0	3.0	6.0			RN associated
	Sc23	17 19 09	-43 35 00	0.78 ± 0.08	-7.31	1.49	6.0	2.0	5.0			
	Sc24	17 21 42	-40 13 48	1.94 ± 0.10	-9.28	0.66	4.0	0.5	6.0			
	Sc25*	17 22 59	-36 17 30	6.0	5.0	5.0			
	Sc26	17 24 49	-36 33 48	4.0	2.0	5.0			
	Sc27	17 27 02	-43 06 12	1.62 ± 0.09	-13.28	1.19	2.0	2.0	6.0			
	Sc28*	17 31 53	-33 30 42	4.0	3.0	6.0			
	Sc29	17 34 32	-38 31 36	0.09 ± 0.09	6.0	2.0	6.0			
	Sc30	17 35 36	-39 14 42	0.22 ± 0.06	-4.24	1.88	5.0	4.0	5.0			
	Sc31	17 42 43	-36 41 42	3.31 ± 0.08	7.02	0.82	4.0	2.0	5.0			
	Sc32	17 44 23	-43 42 12	3.67 ± 0.08	7.73	0.99	6.0	3.0	6.0			S194
Cor. Austr....	CoA1*	18 57 00	-37 02 24	6.32 ± 0.10	6.29	1.00	1.76 ± 0.08	6.14	0.72	35.0	12.0	6.0			S195
	CoA2*	18 58 29	-37 03 12	7.23 ± 0.09	5.68	1.50	1.72 ± 0.09	5.65	1.18	4.0	4.0	6.0			Neb. assoc.
	CoA3	18 58 36	-37 21 00	5.80 ± 0.11	6.03	1.24	1.06 ± 0.09	6.01	0.93	9.0	6.0	6.0			
	CoA4	18 59 44	-37 21 00	3.80 ± 0.08	5.31	0.87	12.0	3.0	6.0			In DC 359.8 - 17.9
	CoA5	19 00 33	-37 29 00	4.19 ± 0.09	5.53	1.38	12.0	6.0	6.0			In DC 359.8 - 17.9, S39
	CoA6	19 03 28	-37 18 24	2.67 ± 0.09	5.21	0.81	16.0	5.0	6.0			Neb assoc.
	CoA7*	19 06 54	-37 12 24	0.82 ± 0.09	4.23	0.47	16.0	7.0	6.0			Neb assoc., S39
	CoA8	19 09 59	-38 17 24	2.29 ± 0.08	5.79	1.03	22.0	7.0	5.0			Neb assoc.
	CoA9	19 11 02	-36 57 06	0.61 ± 0.09	6.64	0.50	16.0	5.0	6.0			Neb assoc.
	CoA10	19 13 04	-36 41 12	3.00 ± 0.06	5.69	0.85	14.0	4.0	6.0			Neb assoc.
	CoA11	19 25 38	-37 40 42	0.10 ± 0.10	5.0	4.0	3.0			Neb assoc.
	CoA12	19 29 35	-37 25 12	0.08 ± 0.08	3.0	3.0	3.0			Neb assoc.
	CoA13	19 30 05	-37 37 24	0.08 ± 0.08	4.0	3.0	3.0			Neb assoc.

NOTE—Units of right ascension are hours, minutes, and seconds, and units of declination are degrees, arcminutes, and arcseconds. The visual extinction data for Vela was obtained from Hetem et al. 1988. An asterisk attached to the name of a condensation means that there is at least one PMS object associated with it. "CG" means cometary globule, "RN" reflection nebula, "DC" dark cloud in the Hartley et al. 1986, 1988 catalog, "HH" Herbig-Haro object, and "S" object in the Sandqvist & Lindros 1976 and Sandqvist 1977 catalogs.

^a Complex spectra.

TABLE 1B

OBSERVED CONDENSATIONS IN SOUTHERN HEMISPHERE CLOUDS: LUPUS COMPLEX

CLOUD	CONDENSATION NAME	RA(1950)	decl.(1950)	¹³ CO ($J = 1-0$)				¹⁸ O ($J = 1-0$)				OPTICAL SIZE			
				T_A^* (K)	V_{LSR} (km s ⁻¹)	ΔV (km s ⁻¹)	T_A^* (K)	V_{LSR} (km s ⁻¹)	ΔV (km s ⁻¹)	l (arcmin)	b (arcmin)	A_V (mag)	COMMENTS		
Lupus 1	Lu1*	15 36 17	-34 36 39	4.67 ± 0.11	4.57	0.75	2.13 ± 0.05	4.50	0.52	10.0	3.5	3.0	Sz 65		
	Lu2	15 36 45	-34 33 09	4.64 ± 0.12	4.86	0.67	1.91 ± 0.04	4.78	0.47	3.5	2.5	3.5			
	Lu3	15 37 00	-33 30 27	4.19 ± 0.11	5.46	1.73	0.46 ± 0.05	5.59	1.57	8.0	2.0	3.8			
	Lu4	15 37 21	-34 30 01	3.34 ± 0.09	4.94	0.82	1.23 ± 0.05	4.64	0.49	4.5	2.0	3.0			
	Lu5	15 38 53	-33 37 00	3.03 ± 0.09	4.65	1.46	0.66 ± 0.04	4.72	0.72	2.0	2.0	2.0			
	Lu6	15 38 54	-33 41 03	1.89 ± 0.10	4.52	0.94	0.51 ± 0.04	4.47	0.82	2.0	2.0	2.0			
	Lu7	15 39 13	-33 59 30	3.99 ± 0.10	5.16	0.85	1.25 ± 0.04	5.50	0.82	12.0	3.5	1.5			
	Lu8	15 39 24	-33 43 19	4.49 ± 0.11	4.63	1.30	1.10 ± 0.04	4.56	0.72	5.0	2.5	4.6			
	Lu9	15 39 59	-34 04 21	4.24 ± 0.11	5.36	0.84	0.92 ± 0.03	5.29	0.37	2.5	2.5	5.6			
	Lu10*	15 41 55	-34 08 17	3.40 ± 0.10	4.96	0.91	0.80 ± 0.03	4.89	0.59	5.0	3.0	4.0	Sz 68, 69		
	Lu11	15 41 57	-34 46 34	4.37 ± 0.12	4.68	0.77	0.83 ± 0.04	4.72	0.58	7.0	3.5	2.0			
	Lu12	15 42 22	-34 31 32	2.29 ± 0.12	4.59	1.20	0.19 ± 0.19			6.0	1.5	1.4			
	Lu13	15 43 21	-35 04 07	2.29 ± 0.11	4.08	1.61	0.19 ± 0.04	4.31	0.89	7.5	2.0	1.5			
	Lu14*	15 44 41	-35 03 35	3.42 ± 0.10	4.37	1.05	0.29 ± 0.05	4.06	0.61	5.0	2.5	1.5	Sz 73, 74		
	Lu15	15 39 51	-33 59 36	5.20 ± 0.10	5.20	1.13	0.76 ± 0.02	5.15	0.97			
	B228	Lu15	15 52 16	-37 38 43	4.92 ± 0.10	4.79	0.63	4.5	2.0	1.5		
Lupus 2	Lu16	15 53 24	-37 48 08	4.89 ± 0.10	4.79	0.76	1.04 ± 0.10	4.97	0.47	3.5	2.0	3.3			
	Lu17*	15 53 18	-37 42 26	2.02 ± 0.11	4.65	1.46	0.83 ± 0.05	4.37	0.58	2.5	2.0	1.8			
	Lu18	15 53 52	-37 41 02	3.88 ± 0.09	4.60	0.79	0.89 ± 0.05	4.59	0.44	5.0	2.5	3.0			
	Lu19	15 55 24	-37 31 34	3.21 ± 0.09	4.71	0.42	0.57 ± 0.06	4.57	0.50	2.5	2.5	2.0			
	Lu20	15 57 54	-37 23 26	3.75 ± 0.11	4.53	0.62	0.94 ± 0.05	4.46	0.47	4.5	2.5	2.8			
	Lu21	15 58 44	-37 14 50	3.87 ± 0.11	4.01	0.84	1.08 ± 0.06	3.98	0.67	3.5	1.5	1.7			
	Lu22	15 56 16	-42 13 39	3.39 ± 0.11	4.69	0.78	0.31 ± 0.06	4.78	0.38	7.0	3.5	1.5			
	Lu23	15 57 31	-41 56 31	4.20 ± 0.10	4.51	0.85	1.24 ± 0.05	4.45	0.57	10.0	2.5	4.0			
	Lu24*	15 56 52	-41 55 20	4.09 ± 0.10	4.35	0.55	0.82 ± 0.04	4.29	0.40	13.0	13.0	1.5			
	Lu25	15 59 11	-41 34 08	4.85 ± 0.09	4.79	0.48	0.55 ± 0.03	4.72	0.42	8.0	2.5	2.0			
	Lu26	16 00 44	-41 52 28	5.23 ± 0.09	4.84	0.69	1.13 ± 0.05	4.79	0.53	1.5	1.5	1.4			
	Lu27	16 03 01	-41 40 42	4.78 ± 0.11	4.89	0.54	0.96 ± 0.06	4.84	0.51	7.0	2.5	1.5			
	Lu28	16 04 57	-41 32 20	3.59 ± 0.11	5.05	0.87	0.21 ± 0.05	4.74	1.15	4.5	1.5	2.2			
	Lu29	16 02 36	-39 17 14	5.00 ± 0.11	5.48	0.91	0.96 ± 0.06	5.52	0.66	2.0	2.0	1.5			
	Lupus 3	Lu30	16 04 29	-39 03 14	3.17 ± 0.07	4.40	0.68	0.26 ± 0.06	4.47	0.72	2.0	2.0	3.0		
		Lu31*	16 05 47	-38 56 02	1.48 ± 0.10	4.44	1.12	0.44 ± 0.04	4.58	0.43	5.0	3.0	2.2	Sz 114	
Lu32		16 06 57	-39 04 28	4.32 ± 0.09	4.42	0.85	0.31 ± 0.04	4.42	0.69	5.0	3.0	3.3			
Lu33		16 07 05	-38 57 30	5.08 ± 0.11	4.86	0.75	1.17 ± 0.04	4.85	0.55	12.0	3.0	3.5			
Lu34		16 07 54	-38 54 53	0.97 ± 0.12	4.90	1.00	0.47 ± 0.04	4.76	0.43	1.5	1.5	1.8			
Lu35		16 08 14	-38 56 35	4.39 ± 0.10	4.99	0.60	0.62 ± 0.04	4.94	0.69	2.0	2.0	3.0			
Lu36		16 08 06	-38 52 37	4.62 ± 0.11	5.09	0.76	1.19 ± 0.05	5.02	0.53	3.0	2.0	1.5			

NOTE—Units of right ascension are hours, minutes, and seconds, and units of declination are degrees, arcminutes, and arcseconds. The coordinates and sizes of the condensations were determined by eye from the ESO J plates. Details on the procedure are given in Vilas-Boas et al. 1994. The visual extinction data were obtained from Andreazza & Vilas-Boas 1995. “Sz” indicates T Tauri stars identified by Schwartz 1977.

15 dark molecular clouds analyzed in this paper; (2) that the condensations in Scorpius seem to be distributed in a shell expanding with velocity smaller or equal to 15 km s^{-1} , in good agreement with large scale H I observations; (3) that Corona Australis has velocity gradients ranging from $-0.5 \text{ km s}^{-1} \text{ pc}^{-1}$ in one extreme to $0.1 \text{ km s}^{-1} \text{ pc}^{-1}$ in the other; and (4) that the four Lupus filaments share similar kinematic properties, suggesting that they originated from the same parental cloud.

2. SOURCE SELECTION

The positions observed in this survey toward Vela, Norma, Lupus, and Carina are regions of visual extinction higher than 2 mag located in complexes of obscuration. The procedure for selecting these positions is described in detail by VMF, and the position accuracy is roughly $1'$. The positions toward Scorpius and Corona Australis were obtained from the Catalog of Southern Dark Clouds (CSDC), compiled from visual inspection of ESO J plates (Hartley et al. 1986). The positions of the peaks are accurate to about $10''$. Almost all condensations selected are class A, which corresponds approximately to a Lynds lower limit opacity of 6 mag (Lynds 1962). The positions toward Vela observed in this survey were obtained from Hetem, Sanzovo, & Lepine (1988).

3. CO OBSERVATIONS

The ^{13}CO and C^{18}O ($J = 1-0$) line observations toward Lupus, Corona Australis, Norma, Vela, Scorpius, and Carina were made in 1992 October and 1993 May. These observations were made with the 15 m Swedish-ESO Submillimeter Telescope (SEST) at La Silla, Chile. The receiver front end was based on a Schottky diode waveguide mixer followed by an intermediate-frequency amplifier. The SSB system temperature was typically 390 K.

The back end used an acousto-optical spectrometer with resolution 43 kHz (0.11 km s^{-1}) and total bandwidth of 100 MHz. The spectra were taken by using overlap frequency switching mode (with 7 MHz frequency shift) and integrating, on average, for periods of 2 minutes. The observations were chopped against a cold load to obtain the correction for atmospheric attenuation. Two independent receivers were used to obtain independent spectra, which were recorded after every minute of integration time. As shown in Tables 1A, 1B and 2 in the next section, the signal-to-noise ratio for the sources with positive ^{13}CO and C^{18}O ($J = 1-0$) detection is on average higher than 10. The half-power beam width was $48''$ and we adopted a beam efficiency of 0.9, as determined by Gredel, van Dishoeck, & Black (1994) observing the Moon. This beam efficiency was adopted because the average optical sizes of the condensations are larger than 3 times the beam size. The rms pointing accuracy is better than $10''$ and was checked systematically by observing SiO masers from VY CMa, IK Tau, and R Cra. The ^{13}CO and C^{18}O results presented in this paper were obtained only from one receiver ("A") since the other receiver ("B") showed a systematic difference of 0.2 km s^{-1} in radial velocity when the spectra obtained with both receivers are compared (see VMF).

4. DATA REDUCTION

The spectra were reduced using the Continuum and Line Analysis Single-Dish Software (Forveille, Gilloteau, & Lucas 1989). Each spectral line was fitted with a Gaussian

function. Some spectra had double-peaked line profiles. In order to distinguish splitting due to saturation effects from splitting due to different sources along the line of the sight, ^{13}CO lines split by less than 0.7 km s^{-1} were considered double only if the C^{18}O line is also double peaked. In order to estimate the peak intensity, line width, and radial velocity of the spectral lines, the fitted baseline was subtracted from the observed spectra. The line parameters were then used to derive the optical depth at the peak of the line, the excitation temperature, and the column density of C^{18}O in the clouds. The method and assumptions used to derive these parameters are discussed in VMF and MLB. These procedures were used to obtain the most homogeneous data possible, in order to allow the results to be directly compared with those of MLB and VMF.

5. OBSERVATIONAL RESULTS

The observational results obtained toward 107 condensations in Lupus, Corona Australis, Norma, Scorpius, Vela, and Carina are shown in Tables 1A and 1B. T_A is the peak antenna temperature corrected for atmospheric attenuation. The uncertainty in antenna temperature corresponds to the rms of the data with respect to the fitted base line. In the last column, "CG" means cometary globules, "RN" means reflection nebulae, "S" with a number attached refers to the catalogs of Sandqvist & Lindros (1976) and Sandqvist (1977), "DC" followed by Galactic coordinates means dark clouds in the Hartley et al. (1986) catalog, and "HH" means Herbig-Haro objects. The T Tauri stars identified by Schwartz (1977) are represented by "Sz" followed by a number. The asterisks attached to the condensation names means that these sources have associated pre-main-sequence objects selected according to the criteria discussed in § 7.1.

Among the clouds observed in this survey, Norma is the only one without any C^{18}O observation, and Carina has only one position observed.

6. DERIVED PARAMETERS OF THE SOURCES

The derived parameters of the condensations observed in this survey are presented in Table 2, where τ is the optical depth and L and M are the equivalent optical diameter and mass, respectively, of the condensation.

To estimate the molecular hydrogen column density, we used the gas-to-dust relation of Bohlin, Savage, & Drake (1978) and the relation between $N(\text{C}^{18}\text{O})$ and A_V obtained by Frerking, Langer, & Wilson (1982). For the Lupus complex this relation was explored in detail using the derived C^{18}O column density and the visual extinction obtained from star counts by Andreazza & Vilas-Boas (1996, hereafter AV).

Figure 1 shows the C^{18}O column density versus visual extinction for 22 condensations observed in Lupus. The dotted and solid lines are relations obtained for Musca and Taurus by VMF and Frerking et al. (1982), respectively. The visual extinctions obtained by AV were modified in two ways for the analysis presented here. First they were increased by 1 mag to account for the extinction of the AV reference field. Second, the more accurate estimates from the Hartley et al. were substituted in the five cases for which the two studies overlapped. For these adopted values of A_V and the observed values of $N(\text{C}^{18}\text{O})$, the Frerking et al. (1982) relation better fits the $N(\text{C}^{18}\text{O})$ versus A_V data and

TABLE 2
DERIVED PARAMETERS OF THE CONDENSATIONS

Condensation Name	$\tau(\text{C}^{18}\text{O})$	T_{EX} (K)	$N(\text{C}^{18}\text{O})$ (10^{15} cm^{-2})	$N(\text{H}_2)$ (10^{21} cm^{-2})	L (pc)	M (M_{\odot})
Vela (450 pc)						
V28	<0.1	10	0.8	6	0.3	10.8
Carina (150 pc)						
Car1	0.37	9	1.4	10	0.2	12.2
Lupus 1 (140 pc)						
Lu1	0.57	9	2.1	14	0.2	17.5
Lu2	0.48	9	1.8	12	0.1	3.8
Lu3	<0.1	10	0.7	6	0.2	3.3
Lu4	0.39	8	1.0	7	0.1	2.3
Lu5	<0.1	12	0.5	4	0.1	0.6
Lu6	0.2	7	0.5	4	0.1	0.6
Lu7	0.28	9	1.1	8	0.3	11.7
Lu8	0.14	12	1.0	7	0.1	3.0
Lu9	<0.1	16	0.3	3	0.1	0.7
Lu10	0.12	11	0.7	5	0.2	3.1
Lu11	<0.1	10	0.5	4	0.2	3.7
Lu13	<0.1	10	0.2	2	0.2	1.3
Lu14	<0.1	10	0.2	2	0.1	1.0
B228	<0.1	10	0.7	6
Lupus 2 (140 pc)						
Lu16	<0.1	10	0.5	7	0.1	1.8
Lu17	0.48	6	0.7	8	0.1	1.4
Lu18	0.11	13	0.8	8	0.1	3.5
Lu19	<0.1	10	0.3	3	0.1	0.7
Lu20	0.16	11	0.8	8	0.1	3.5
Lu21	0.21	9	0.9	9	0.1	1.6
Lupus 4 (140 pc)						
Lu22	<0.1	10	0.1	2	0.2	1.8
Lu23	0.15	10	1.1	9	0.2	8.6
Lu24	<0.1	10	0.3	6	0.5	35.5
Lu25	<0.1	10	0.2	3	0.2	2.0
Lu26	<0.1	19	0.6	7	0.1	0.6
Lu27	<0.1	27	0.5	7	0.2	4.3
Lu28	<0.1	10	0.3	3	0.1	0.7
Lupus 3 (140 pc)						
Lu29	<0.1	10	0.6	5	0.1	0.7
Lu30	<0.1	10	0.2	2	0.1	0.3
Lu31	0.25	6	0.3	6	0.2	3.2
Lu32	<0.1	10	0.2	3	0.2	1.4
Lu33	0.11	15	1.3	10	0.2	13.6
Lu34	0.62	5	0.5	6	0.1	0.5
Lu35	<0.1	10	0.4	4	0.1	0.5
Lu36	0.17	12	0.6	7	0.1	1.6
Scorpius (145 pc)						
Sc2	<0.1	10	0.5	4	0.1	0.8
Sc3	<0.1	10	0.3	3	0.1	1.6
Sc4	<0.1	10	0.5	4	0.1	0.5
Sc6	<0.1	10	0.4	3	0.1	0.3
Sc11	0.42	10	2.0	13	0.2	8.0
Sc12	<0.1	10	0.6	5	0.2	4.9
Sc13	0.37	8	1.2	10	0.2	7.7
Sc14	<0.1	10	0.5	4	0.1	0.3

TABLE 2—Continued

Condensation Name	$\tau(\text{C}^{18}\text{O})$	T_{EX} (K)	$N(\text{C}^{18}\text{O})$ (10^{15} cm^{-2})	$N(\text{H}_2)$ (10^{21} cm^{-2})	L (pc)	M (M_{\odot})
Sc18	<0.1	10	0.6	5	0.1	1.6
Sc19	<0.1	10	0.4	3	0.1	0.5
Sc20	<0.1	10	0.3	3	0.2	3.4
Sc22	<0.1	10	1.9	12	0.2	7.2
Corona Australis (130 pc)						
CoA1	0.21	14	1.8	13	0.8	167.2
CoA2	0.13	19	2.2	14	0.2	7.3
CoA3	<0.1	10	1.2	8	0.3	14.2

NOTE—The molecular hydrogen column density was calculated using the Frerking et al. 1982 relation. After the name of each cloud is given its distance, from Sahu 1992 (Vela), Hetem et al. 1988 (Carina), Hughes & Hartigan 1993 (Lupus), De Geus 1988 (Scorpius), or Andreazza & Vilas-Boas 1996 (Cor. Australis).

was used to obtain a relation between the H_2 and the C^{18}O column densities.

To estimate the molecular hydrogen volume density, we used the $N(\text{H}_2)$ and the equivalent optical size of the condensation given by $(l \times b)^{0.5}$, where l and b are the semi-major and semiminor optical sizes, respectively. The corresponding maximum mass of the condensations was estimated using equation (10) from VMF, which assumes the condensations as uniform spheres. The mass uncertainty is higher than a factor of 2, primarily because of uncertainties in the factor used to convert from C^{18}O to molecular hydrogen column density and to uncertainties in the source distances.

There are 30 positions in Table 2, where the C^{18}O optical depths are given as smaller than 0.1. For these positions, either the optical depths are comparable to their own uncertainty or the ^{13}CO to C^{18}O line intensity ratios are larger

than 5.5. Values of intensity ratios greater than 5.5 can not be consistent with the single excitation temperature model used to analyze the data (MLB).

These high ratios could be related to different ^{13}CO and C^{18}O excitation temperatures or fractionation or due to some selective mechanism destroying more ^{13}CO than C^{18}O . B228 in Lupus 1, where the ^{13}CO to C^{18}O ratio is roughly 7, is a good example: It has the highest ^{13}CO antenna temperature among the 15 positions observed in Lupus 1. However, its C^{18}O temperature is smaller than observed toward 7 other positions in this cloud. For these positions the C^{18}O column density was estimated using the equation $N(\text{C}^{18}\text{O}) = [(8\pi\nu^2k)/(hc^3 A_{1-0})]U(T_{\text{ex}}) \int T_a^*(\nu) d\nu$, which is valid for optically thin lines, where $T_a^*(\nu)$ is the antenna temperature along the line profile, and $U(T_{\text{ex}})$ is the classical partition function estimate assuming the excitation temperature 10 K. We also estimate that the column densities derived in this manner are uncertain by no more than a factor of 2.

7. MAIN OBSERVATIONAL PROPERTIES OF THE DARK CLOUDS

In this section we compare the average properties of the condensations of the dark clouds observed in MLB, VMF, and this survey. The data accumulated from these surveys cover almost all known nearby dark clouds within a few hundred parsecs, and they form a homogeneous sample. In order to compare the properties of these clouds we will consider the line widths, excitation temperature, and the C^{18}O and H_2 column densities. Among these parameters the H_2 column density is the most uncertain because of uncertainties in converting from CO to H_2 , in the shape of the condensations, and in the distance of the sources.

The average values of the observed parameters are shown in Table 3. Errors shown are rms. F in the final column is the fraction of condensations with pre-main-sequence objects associated. The average excitation temperature for Lup 2, 3, 4, and Corona Australis are not given in this table because of the small number of positions in these clouds for which the excitation temperature could be determined.

Among the clouds in Table 3, the average C^{18}O column density is greater than $2 \times 10^{15} \text{ cm}^{-2}$ in Ophiuchus, equal to $1.6 \times 10^{15} \text{ cm}^{-2}$ in Taurus and smaller or equal to $1 \times 10^{15} \text{ cm}^{-2}$ for the other clouds.

The three positions observed in Corona Australis with positive C^{18}O detection are located in an extended filament

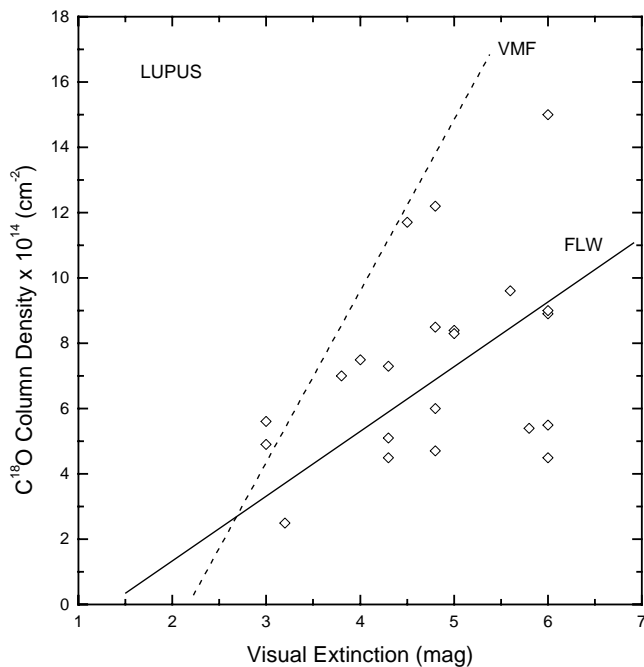


FIG. 1.— C^{18}O column density vs. visual extinction for the positions observed toward the Lupus complex. The solid and dashed lines are column density vs. extinction obtained by Frerking et al. (1982, “FLW”) and VMF in Musca, respectively.

TABLE 3
AVERAGE VALUES OF CONDENSATION LINE DATA FROM MLB, VMF, AND THIS SURVEY

Cloud	Number of Condensations in $^{13}\text{CO}/\text{C}^{18}\text{O}$	$\Delta V(^{13}\text{CO})$ (km s^{-1})	$\Delta V(\text{C}^{18}\text{O})$ (km s^{-1})	$N(\text{C}^{18}\text{O})$ (10^{15} cm^{-2})	T_{EX} (K)	$N(\text{H}_2)$ (10^{21} cm^{-2})	F
Taurus	26/26	1.0 ± 0.3	0.6 ± 0.2	1.6	10 ± 2	10.0 ± 6	0.63
Ophiuchus	14/14	1.9 ± 1.0	0.8 ± 0.4	2.6	14 ± 3	14.0 ± 10	0.47
Cepheus	06/06	1.3 ± 0.4	0.6 ± 0.2	1.1	9 ± 2	7.0 ± 2	0.80
Vela ^a	26/19	0.7 ± 0.2	0.6 ± 0.2	0.5	12 ± 2	5.0 ± 2	0.13
Musca	16/13	0.8 ± 0.2	0.5 ± 0.1	0.8	10 ± 4	3.0 ± 1	0.06
Coalsack ^b	8/6	0.8 ± 0.2	0.6 ± 0.1	0.5	10 ± 4	4.0 ± 2	... ^c
Cham II	28/10	1.2 ± 0.4	0.7 ± 0.3	0.7	7 ± 2	5.0 ± 2	0.07
Cham III	16/08	1.1 ± 0.3	0.9 ± 0.5	0.6	7 ± 1	3.0 ± 2	0.00
Lupus 1	15/14	1.1 ± 0.3	0.7 ± 0.3	0.8	10 ± 3	6.0 ± 3	0.21
Lupus 2	07/06	0.8 ± 0.3	0.5 ± 0.1	0.6	...	7.0 ± 2	0.14
Lupus 3	08/08	0.8 ± 0.2	0.6 ± 0.1	0.5	...	5.0 ± 2	0.13
Lupus 4	07/07	0.7 ± 0.1	0.6 ± 0.2	0.5	...	5.0 ± 3	0.14
Norma ^a	12/00	1.4 ± 0.7 ^c
Scorpius ^a	30/12	1.2 ± 0.6	0.9 ± 0.3	0.8	...	6.0 ± 4	0.19
Cor. Aust.	12/03	0.9 ± 0.2	0.9	1.7	14	12.0	0.23

NOTE—Carina is not included because we observed only one position toward this cloud.

^a For this, the velocity dispersion of the radial velocities is larger than 6 times the velocity dispersion obtained from the average of the observed line widths. Cloud is formed by fragments with different radial velocities.

^b The ^{13}CO data presented in this table for the Coalsack were obtained from VMF, and C^{18}O data are from this survey.

^c There are several *IRAS* point sources with color indexes indicative of pre-main-sequence objects identified toward this cloud.

that is $55' \times 14'$ in size. This filament, known as CrA cloud or condensation A according to AV, is an active site of recent star formation (Graham 1992) and contains the well-known emission-line irregular variable star R CrA. This filament together with ρ Ophiuchus are the clouds with the highest C^{18}O column density among the dark clouds observed in these surveys. Taking into account the uncertainties, the clouds have almost the same average excitation temperatures (≈ 10 K) and C^{18}O line widths (0.7 km s^{-1}). However, the average ^{13}CO line width (1.9 km s^{-1}) observed in Ophiuchus is twice as broad as is observed toward the other dark molecular clouds in these surveys. Since high star formation activity is also observed toward Cepheus and Taurus, the high ^{13}CO line width observed toward Ophiuchus does not seem to be uniquely correlated with high star formation activity.

Another observational result that deserves attention is the dispersion of the ^{13}CO line width. In Ophiuchus it is 1.0 km s^{-1} , 3 times the average dispersion of all clouds (0.32 ± 0.16) in Table 3. If the condensations observed toward Ophiuchus are located in the same cloud, some external mechanism must be acting on Ophiuchus to explain the observed mean ^{13}CO line width and its line width dispersion. This result seems to be compatible with the hypothesis that the overall Ophiuchus morphology is suggestive of the passage of a shock (Vrba 1977; Loren & Wootten 1986; de Geus 1988). The ^{13}CO line widths observed toward dense condensations are always larger than those of C^{18}O and, certainly, measure the turbulence of the condensations and intercondensation gas. Thus, increased turbulence in the intercondensation gas can produce ^{13}CO line widths that are broader than the C^{18}O line widths without producing any measurable effect on the C^{18}O line width or excitation temperature. Small-velocity shocks ($V_s \leq 15 \text{ km s}^{-1}$) are a good mechanism for accelerating gas and producing turbulence. According to de Geus (1992) and Motte, André, & Neri (1998), part of Ophiuchus

is under the action of a small velocity shock wave produced by the upper Scorpius OB2 association. This scenario could explain the high ^{13}CO line width dispersion observed.

Although large dispersions in line width of about 0.7 and 0.6 km s^{-1} are seen in Norma and Scorpius, respectively, the Norma data seem to be contaminated by carbon monoxide emission from clouds far behind, and Scorpius is not a dark cloud but a set of isolated condensations apparently located in an expanding ring (§ 8.3).

The narrowest C^{18}O average line widths and line width dispersions were observed in Lupus 2 and Musca, which have similar C^{18}O column densities. The highest C^{18}O line widths ($\sim 0.9 \text{ km s}^{-1}$) were observed in Corona Australis, Chameleon III, and Scorpius.

7.1. *IRAS* Sources and Young Stellar Objects

A search for infrared sources and young stellar objects was conducted using the *IRAS* Point Source Catalog and surveys of T Tauri and pre-main-sequence (PMS) emission-line stars (Beichman et al. 1984; Schwartz 1977; Whittet, Prust, & Wesselius 1991; Weintraub 1990; Herbig & Bell 1988; Gauvin & Strom 1992; Persi et al. 1990; Chen et al. 1995). The procedure for selecting an *IRAS* point source as a “PMS object” is described in VMF. Condensations with associated *IRAS* sources are listed in Table 4, where d is the distance of the *IRAS* source to the observed position and F_{12} , F_{25} , F_{60} , and F_{100} are the uncorrected flux densities in the four *IRAS* bands. In order to establish the association of the *IRAS* sources with the condensations, we selected only the *IRAS* sources located at a distance from the condensation position less than the smaller optical size of the condensation.

As given in the last column of Table 3, 21% and 13% of the condensations observed toward Lupus 1 and 3, respectively, have associated PMS objects, while 14% of the condensations in Lupus 2 and 4 have associated sources. In Corona Australis 23% of the condensations contain a PMS

TABLE 4
IRAS SOURCES WITH COLOR INDEXES OF PMS OBJECTS

Condensation Name	<i>IRAS</i> Identification	RA(1950)	(1950) decl.	d (arcmin)	$F_{1.2}$ (Jy)	$F_{2.5}$ (Jy)	$F_{6.0}$ (Jy)	F_{100} (Jy)
V28	08242 – 5050	08 24 16.5	–50 50 44	1.3	0.8	6.3	26.1	58.3
V30	08261 – 5100	08 26 11.5	–51 00 39	3.3	0.9	2.5	4.3	10.9
N3	16000 – 5317	16 00 05.6	–53 17 17	3.4	1.4	2.5	3.3	310.0
N5	16094 – 5249	16 09 24.9	–52 49 17	5.5	6.4	8.0	39.8	321.0
N7	16111 – 5051	16 11 06.1	–50 51 08	5.1	2.2	2.9	150.0	229.0
N11	16295 – 4452	16 29 33.1	–44 52 05	0.9	1.2	5.4	27.1	52.8
Sc2	16510 – 4026	16 51 05.7	–40 26 47	0.6	1.0	1.7	15.9	56.8
Sc11	17072 – 4029	17 07 14.3	–40 29 25	1.5	2.7	2.7	16.9	318.0
Sc18	17159 – 3324	17 15 55.0	–33 24 16	0.5	0.6	3.8	16.1	278.0
Sc20	17172 – 4316	17 17 15.9	–43 16 54	1.4	0.4	0.8	4.2	29.0
Sc25	17227 – 3619	17 22 44.5	–36 19 35	3.6	1.7	12.7	74.8	488.0
Sc28	17317 – 3331	17 31 44.4	–33 31 34	2.0	104.0	292.0	234.0	736.0
CoA1	18577 – 3701	18 57 42.9	–37 01 40	8.6	4.9	9.2	18.1	27.9
CoA2	18585 – 3701	18 58 32.9	–37 01 32	1.8	111.0	222.0	608.0	1210.0
CoA7	19063 – 3709	19 06 22.7	–37 09 21	6.9	0.6	1.4	2.2	5.1
Lu1	15362 – 3436	15 36 15.2	–34 36 32	0.4	0.6	0.8	0.4	13.3
Lu10	15420 – 3408	15 42 01.3	–34 08 09	2.1	2.6	4.0	7.9	24.4
Lu17	15534 – 3740	15 53 24.5	–37 40 34	2.3	2.5	4.6	5.0	10.5
Lu24	15573 – 4147	15 57 18.8	–41 47 05	9.6	0.3	0.8	1.2	4.6

NOTE—Units of right ascension are hours, minutes, and seconds, and units of declination are degrees, arcminutes, and arcseconds. The fifth column gives the distance d between the observed position of the condensation, given in Tables 1A and 1B, and the selected *IRAS* sources.

object, while in the other clouds it is less than 20%. As in VMF, here this fraction is used as an indication of the star formation activity. According to this fraction, RCrA and Lupus 1 are the filaments with the highest star formation activity among the clouds observed in this survey. From Table 3 we see that still higher star formation activity is found in Ophiuchus, Taurus, and Cepheus: more than 38% of the positions observed by MLB have associated infrared point sources.

The average values of the $C^{18}O$ and H_2 column densities in Table 3 show that these parameters assume high values when there is high star formation activity, independently of the ^{13}CO and $C^{18}O$ line widths. Selecting the clouds with high star formation activity (Taurus, Ophiuchus, Cepheus, and Corona Australis), we find that the condensations of an active star-forming dark cloud must have average $C^{18}O$ and H_2 column densities higher than 1.8×10^{15} and $1.1 \times 10^{22} \text{ cm}^{-2}$, respectively. For the other clouds, where the star formation activity is low (Vela, Musca, the Coal-sack, Cham II and III, Lupus, and Scorpius), these parameters are $0.6 \pm 0.1 \times 10^{15}$ and $5.0 \pm 1 \times 10^{21} \text{ cm}^{-2}$, respectively. Assuming the typical diameter of the condensation 0.2 ± 0.1 pc, which is the average diameter of all condensations observed, and the average H_2 column density obtained above, we find that the condensations of a cloud must have molecular hydrogen densities larger than $2 \times 10^4 \text{ cm}^{-3}$ in order for it to be an active star-forming cloud.

8. INDIVIDUAL REGIONS

In this section we will discuss some relevant aspects of the clouds observed in this survey. Vela and Scorpius are not dark molecular clouds but a set of condensations spread over extended areas. More than 27 condensations were observed over a large area toward Vela by VMF. In the present survey only a further nine condensations were observed toward this region, corresponding to 25% of all condensations observed in this region by VMF and this

survey. For this reason, this region will not be discussed below. Detailed discussion about the structure of Vela are given by, for example, Zealey et al. (1983), Reipurth (1983), Sahu (1992), and VMF.

8.1. *Lupus*

An extensive survey of ^{12}CO ($J = 1-0$) in *Lupus* with 30' angular resolution was reported by Murphy, Cohen, & May (1986). Gahm, Johansson, & Liseau (1993) presented CO ($J = 1-0$) images of *Lupus* 2 as well as complementary observations in ^{12}CO ($J = 2-1$) and ^{13}CO ($J = 1-0$). Recently this cloud complex was studied using star counts by Andreatza & Vilas-Boas (1996) and Cumbrésy (1999) and ^{13}CO ($J = 1-0$) emission with 3' spatial resolution (Tachihara et al. 1996). A review of the properties of the *Lupus* clouds and their associated young objects was presented by Krautter (1991).

Among the 36 condensations observed in the *Lupus* complex, four in *Lupus* 1 (Lu1, Lu2, Lu7, and Lu8) have $C^{18}O$ column densities $\geq 10^{15} \text{ cm}^{-2}$. Lu1, the densest condensation, has the shape of cometary globules and has two associated T Tauri stars. This condensation and Lu2 are coincident in position with condensation C reported by AV, which is located in an extended structure to the southwest of the main filament. Lu7 and Lu8 are in condensation D and are less than 7'9 from the *IRAS* point source 15398–3559, which is the only deeply embedded pre-main-sequence object (B228 in Table 1B) in the *Lupus* complex. A shock-excited nebulosity has been identified near this *IRAS* source (Heyer & Graham 1989), and a molecular outflow with dynamic timescale of 2×10^3 yr is associated with this object (Tachihara et al. 1996). Our observations toward this object (Table 1B) show the highest ^{13}CO line temperature among all condensations observed in *Lupus*. However its $C^{18}O$ line temperature is very small compared to that in ^{13}CO , yielding high ^{13}CO to $C^{18}O$ antenna temperature

ratios, which is inconsistent with our single excitation temperature model for the emission.

The Lu10 condensation has associated with it two blue-shifted jets and the T Tauri stars Sz68 and Sz69 (Heyer & Graham 1989), which have an associated candidate HH object. This condensation does not show any remarkable characteristic (Table 2). The condensations Lu16 and Lu17, in Lupus 2, are located in condensation A (see AV), which is associated with the object HH 55. Lu 17 is 2' from the extremely active T Tauri star RU Lup and presents a ^{13}CO line width 2 times broader than the other condensations observed in this filament.

In Lupus 4 the condensation Lu24 is coincident with condensation B (see AV), and Lu23, Lu25, and Lu26 are coincident with smaller structures with peak visual extinctions smaller than 3 mag.

In Lupus 3, condensations Lu31 to Lu33 are located in structure A of the extinction map (AV), and Lu34 to Lu36 are in B. The structure A has associated one of the densest T associations known and the two Herbig Ae/Be stars HR 5999 and HR 60000. The observational results do not show any remarkable difference among the observational parameters of the condensations in this region and other parts of the Lupus 3.

Among the filaments observed in the Lupus complex, Lupus 1 has the highest average C^{18}O column densities ($0.8 \times 10^{15} \text{ cm}^{-2}$). Lupus 1 has a star formation rate larger than 20% (Table 3), while this rate is smaller than 15% for the condensations observed in Lupus 2, 3, and 4. According to Tachihara et al. (1996) the star formation efficiency toward Lupus 1 and 3 are 0.4% and 3.8%, respectively.

8.1.1. Velocity Structure

Plots of the ^{13}CO radial velocity versus position for all filaments observed in Lupus are shown in Figure 2. The average radial velocity and velocity dispersion for Lupus 1,

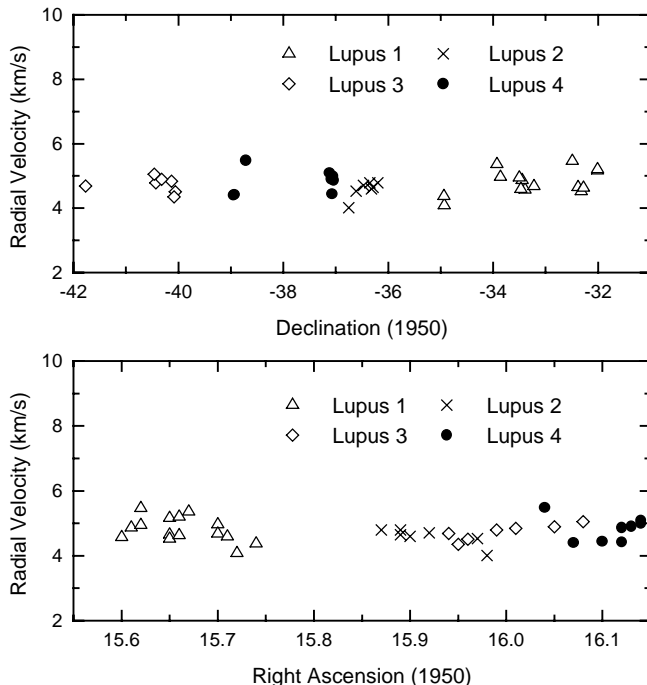


FIG. 2.—Radial velocity vs. right ascension and declination for the condensations observed toward the four Lupus filaments.

2, 3, and 4 are $4.8 \pm 0.4 \text{ km s}^{-1}$, $4.6 \pm 0.3 \text{ km s}^{-1}$, $4.7 \pm 0.3 \text{ km s}^{-1}$, and $4.8 \pm 0.4 \text{ km s}^{-1}$, respectively. This result shows that they have almost the same average radial velocity and velocity dispersion. A similar result is obtained if the velocity dispersion is estimated from the observed line width, suggesting that the complex of filaments share similar kinematic properties and could have originated from the same parental cloud. Although these condensations share similar overall kinematic properties, the radial velocity versus position shows different behavior along the filaments. Lupus 2 and 4 show -0.2 and $0.13 \text{ km s}^{-1} \text{ pc}^{-1}$ velocity gradients, respectively, while there is no significant velocity gradient in Lupus 3. Lupus 1 shows a complex velocity structure (Fig. 3). Three condensations observed in this filament are located in an extended structure to the west of the main filament. These condensations are represented in Figure 3 by empty circles. Linear fits of the velocity position data show that from reference position 0.0 to 0.4 the velocity gradient is $-0.7 \text{ km s}^{-1} \text{ pc}^{-1}$, from 0.4 to 0.8 it is $+0.7 \text{ km s}^{-1} \text{ pc}^{-1}$, and from 0.8 to 2.2 it is $-0.3 \text{ km s}^{-1} \text{ pc}^{-1}$. Detailed maps of the whole filaments with high angular resolution are still necessary to understand their internal velocity structure.

8.2. Norma

The condensations of this cloud have Galactic latitudes between 0° and 2° and are seen against the Galactic plane. No C^{18}O line observation was done toward this cloud. Of the 12 condensations observed in ^{13}CO , seven have radial velocities between -15 and -38 km s^{-1} , which are smaller than the typical radial velocity of the condensations of the nearby dark clouds observed in this and previous CO surveys. Since this cloud is seen against the Galactic plane, it seems that these lines are produced in clouds behind the nearby Norma cloud.

Five of the condensations in Norma have radial velocities of -3 to -5 km s^{-1} , and the strongest ^{13}CO emission was

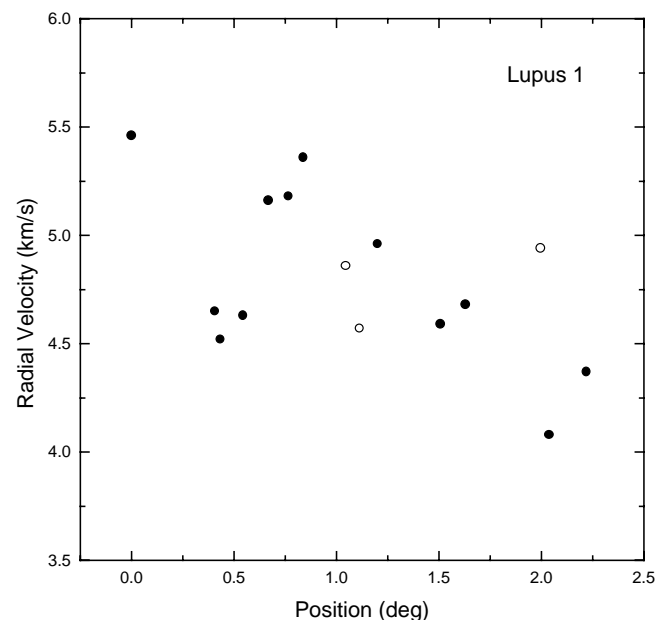


FIG. 3.—Radial velocity vs. position for the condensations observed toward Lupus 1, located along the main filament (filled circles) in an extended structure southwest of this filament (open circles).

observed toward N11. This condensation together with N10 and N12 are located in an isolated cloud cataloged as 187 in the Sandqvist (1977) survey. N11 is 7' from HH 56 and HH 57. A peak of ^{12}CO with similar radial velocity was also observed toward N11 by Alvarez et al. (1986). In this position the ^{13}CO line is 2 times wider than observed in N10, which is 27' away, but still in the same filament (S187). N12 is also 26' to the south of N11 but has -23.3 km s^{-1} radial velocity, suggesting that this emission comes from a different region. According to Alvarez et al. (1986) no velocity gradient was observed in ^{12}CO ($J = 1-0$) toward this cloud. The ^{13}CO radial velocity between N10 and N11 shows $-0.25 \text{ km s}^{-1} \text{ pc}^{-1}$, assuming that the cloud is located at a distance of 700 pc (Graham & Frogel 1985). Distances for this cloud of around 200 pc have been proposed by Cohen & Schwartz (1984) and Hetem et al. (1988). Detailed maps of ^{13}CO and C^{18}O are necessary to understand the motions of these condensations.

8.3. Scorpius

The condensations selected toward this region are not part of a dark cloud or filament. Rather, they are small condensations spread over an extended area and forming a set of 32 isolated condensations with visual extinctions bigger than 6 mag and optical sizes smaller than 6'. They were selected from the CSDC catalog and are in the $l = 344^\circ\text{--}347^\circ$ and $b = 6^\circ\text{--}8^\circ$ Galactic coordinate interval. The space distribution of part of these condensations is coincident with large-scale H I structures that dominate the appearance of the fourth Galactic quadrant outside the Galactic plane (Blaauw 1964; de Geus 1988). These H I structures or loops are substructures associated with three subgroups of the Scorpio-Centaurus OB association (Blaauw 1964; Weaver 1978; de Geus 1988).

This set of condensations has the largest $^{13}\text{CO}/\text{C}^{18}\text{O}$ ratio among all regions observed in MLB, VMF, and this survey. Among the 12 condensations observed in C^{18}O , three (Sc11, Sc13, and Sc22) have C^{18}O column densities larger than $1 \times 10^{15} \text{ cm}^{-2}$, and only two (Sc11, Sc13) have $\tau(\text{C}^{18}\text{O}) \geq 0.1$. As in Norma, the velocities are diverse and only 10 condensations have radial velocities in a range small enough ($5\text{--}8 \text{ km s}^{-1}$) to suggest that they are at about the same distance.

Considering all condensations observed in C^{18}O , we find that Scorpius has a larger average column density than is observed toward Vela, which is a set of more than 25 isolated cometary globules located in an expanding shell (Zealey et al. 1983; Reipurth 1983; Hartley et al. 1986).

According to the CSDC (Hartley et al. 1986), there is only one cometary globule (Sc2) among the condensations observed toward Scorpius.

8.3.1. Velocity Structure

The velocity distribution of the condensations observed in this region is shown in Figure 4, where there are two peaks with radial velocities between -6.0 to -9.0 km s^{-1} and $+6.0$ to $+9.0 \text{ km s}^{-1}$. This figure also shows that there are 2 times more condensations (20) with positive radial velocities than negative (10), and the upper and lower radial velocity limits are $+15$ and -18 km s^{-1} , respectively. With the assumption that these condensations are in a uniformly expanding shell, the velocity distribution in Figure 4 suggests a maximum expansion velocity 18 km s^{-1} . An average expansion velocity of about 7.5 km s^{-1} was also estimated

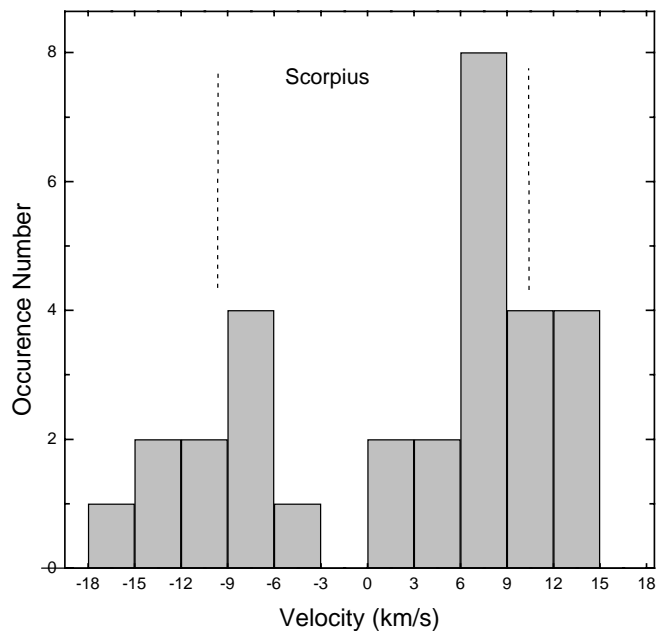


FIG. 4.—Histogram of the radial velocity distribution observed toward Scorpius. Two peaks with radial velocities around -7.5 and 7.5 km s^{-1} are seen. The dotted lines show a model of an expanding ring with an expansion velocity of 10 km s^{-1} (de Geus 1988).

by fitting two Gaussians to the peaks of the velocity distribution given in Figure 4. In this figure the dashed lines are the radial velocities expected if the condensations were located in a shell with 10 km s^{-1} constant expansion velocity. This is the velocity obtained by de Geus (1988) in fitting models of expanding shells to the observed H I maps surrounding the Upper Scorpius and Upper Centaurus-Lupus OB associations. Although these H I structures dominate the appearance of the fourth Galactic quadrant, Cappa de Nicolau & Pöppel (1986) showed that there is evidence that these H I shells extend from $b = 50^\circ$ to -40° . According to de Geus (1988) the region containing the Upper Scorpius region and Ophiuchus was originally filled with a bigger cloud at velocities comparable to the velocity observed in Ophiuchus (4 km s^{-1}) today. Because of the massive star formation activity and supernovae in these associations, an expanding bubble with expansion velocity of $10\text{--}15 \text{ km s}^{-1}$ was formed. This bubble accelerated the neighboring gas such that the negative velocities mark the approaching side of the expanding H I shell, which has passed through gas of relatively low density.

The densest condensations in Scorpius observed in this work (Sc11 and Sc13) have radial velocities close to $+6 \text{ km s}^{-1}$, while the other condensations, with smaller column densities, are spread in the radial velocity interval between -18 and 15 km s^{-1} . If these condensations were accelerated from their original speed by a shock wave, the velocity peaks at -7.5 and $+7.5 \text{ km s}^{-1}$ suggest that the preshock gas had a radial velocity around 0 km s^{-1} and then expanded into a medium with uniform density.

8.4. Corona Australis

The Corona Australis dark cloud is a complex of nine regions identified in extinction-distribution maps (Rossano 1978; AV; Cumbrésy 1999). One of these regions (condensation A according to AV, also known as CrA

cloud) is a dense and highly elongated filament that is a region of very recent star formation (Graham 1992) and hosts the well-known emission-line irregular variable star R CrA. Associated with this condensation are several Herbig-Haro objects and a number of faint and bright infrared sources (Reipurth & Graham 1988; Strom, Grasdalen, & Strom 1974; Cohen & Schwartz 1984; Taylor & Storey 1984; Wilking et al. 1992). This is the most active star-forming filament in this cloud, and several molecular line observations have been done toward this filament (Loren 1979; Goss et al. 1980; Harju et al. 1993). According to Harju et al. (1993) the star formation efficiency in this filament is around 0.40.

In this survey, five positions were observed in the CrA cloud (CoA1 to CoA5), and the other positions are coincident with structures B through F in the extinction map presented by AV. CoA2 has three embedded stars and two T Tauri stars associated with it and the highest C^{18}O column density among all condensations observed in this survey. Detailed C^{18}O maps and discussion of the central part of CrA, which is coincident with CoA2, were presented by Harju et al. (1993). These show that this condensation is complex, with at least two subcondensations and several PMS objects associated with it. The condensation CoA4 has associated with it two infrared sources and one T Tauri star, and in C^{18}O it contains two subcondensations (Harju et al. 1993). All the other condensations observed in this survey are located outside the region mapped by Harju et al. and Loren (1979).

CoA7, which is C in AV and B in Rossano (1978), has a PMS object associated (Persi et al. 1990). The other positions have ^{13}CO antenna temperature smaller than 3.5 K, which together with low visual extinction suggest they are not dense objects. Also, there is not any PMS object associated with these condensations.

8.4.1. Velocity Structure

Figure 5 shows ^{13}CO velocity versus position for the condensations observed in Corona Australis (*open circles*). CoA1 was used as reference to calculate the positions of the condensations. The solid lines are linear regression fits to the ^{13}CO data. Between the positions 0 and 80 the velocity gradient is $-0.5 \text{ km s}^{-1} \text{ pc}^{-1}$, while between 75 and 200 it is $+0.1 \text{ km s}^{-1} \text{ pc}^{-1}$. Similar velocity gradients are also identified in the high velocity resolution profile of the 1667 MHz OH line observed toward 12 positions by Cappa de Nicolau & Pöppel (1991), represented in Figure 5 by crosses. Toward CoA6 and CoA8 the ^{13}CO lines are split into two components separated by roughly 1.7 km s^{-1} . The average radial velocity of the condensations in this cloud ($5.5 \pm 0.5 \text{ km s}^{-1}$) is the same as the average radial velocity of an intense ridge of H I emission (Schober 1976; Burton & Lutz 1983) extending from $b = -40^\circ$ to -10° , having roughly constant radial velocity (6 km s^{-1}) from -10° to -40° and decreasing toward higher Galactic latitudes. This H I ridge is a local object of very large angular extension having a peculiar velocity distribution that is quite different from the one expected for gas moving in circular Galactocentric orbits (Cappa de Nicolau & Pöppel 1991).

The gas distribution around the subgroups of Scorpius-Centaurus (de Geus 1988) suggests that this H I ridge is the southern part of a large H I loop centered on $(l, b) = (320^\circ, 10^\circ)$ and associated with the Upper Centaurus-Lupus association. This result seem to agree with the Sandquist &

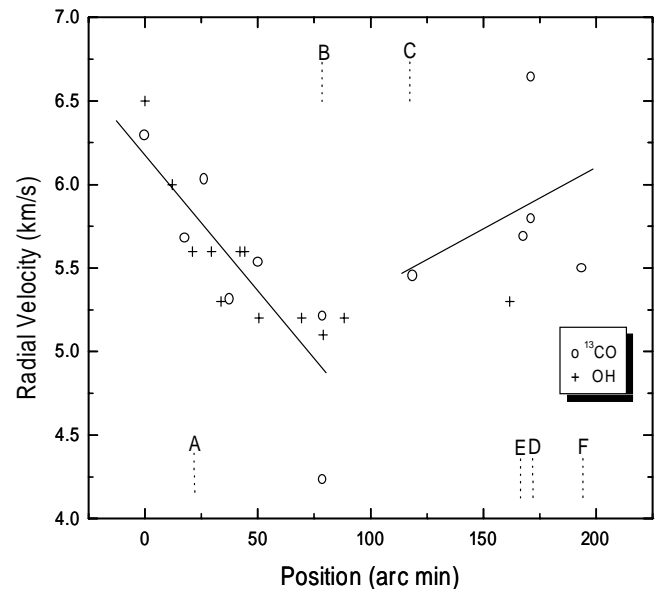


FIG. 5.—Radial velocity vs. position for the condensations observed toward Corona Australis, showing ^{13}CO radial velocities observed in this survey (*open circles*), OH radial velocities observed by Cappa de Nicolau & Pöppel (1991; *crosses*), and the positions of the structures A to F defined by AV as regions with visual extinction higher than 3 mag (*vertical dashed lines*).

Lindros (1976) picture, in which the Corona Australis molecular cloud could be the result of a density inhomogeneity accreted in an expanding gas shell.

8.5. Carina

This condensation seems to be remnant of a large cloud that may have disrupted after the formation of the open cluster IC 2606. The Carina cloud is located at about the same distance as the Coalsack cloud, and on large-scale view of the Galaxy it appears to be connected with this cloud (Hetem et al. 1988). This cloud shows very narrow ^{13}CO and C^{18}O line widths when compared to the other condensations observed in this survey and has a radial velocity that is the same as is observed toward the Coalsack.

9. SUMMARY AND CONCLUSIONS

This paper presents ^{13}CO and C^{18}O ($J = 1-0$) line observations toward more than 100 condensations in Scorpius, Vela, Norma, Carina, and the dark molecular clouds Lupus and Corona Australis. The findings of MLB, VMF, and this survey are compared, and the mean observational results are discussed individually for each cloud in order to describe the dynamic properties of each dark cloud. The main results of this survey are as follows.

1. The most opaque condensations in dark clouds with high star formation activity (Ophiuchus, Taurus, Cepheus, and Corona Australis) have average C^{18}O and H_2 column densities of 1.8×10^{15} and $1.1 \times 10^{22} \text{ cm}^{-2}$, respectively. If the average size of such a condensations is $\leq 0.2 \text{ pc}$, it must have average H_2 number density $\geq 10^4 \text{ cm}^{-3}$ to form stars.

2. The condensations of the main filament of Ophiuchus have an average ^{13}CO line width of 1.9 km s^{-1} , roughly twice as large as the average for all the other 14 dark clouds

listed in Table 3. Also, the line width dispersion (1.0 km s^{-1}) of these condensations in Ophiuchus is 3 times larger than the average value ($0.3 \pm 0.2 \text{ km s}^{-1}$) in the other dark clouds.

3. Among the 36 condensations observed in Lupus, only Lupus 1 shows recent star formation activity.

4. The four Lupus filaments have almost the same radial velocity and velocity dispersion, indicating that they share similar kinematic properties and could have originated from the same parental cloud.

5. The least dense condensations were observed toward Scorpius. The distribution of radial velocities of the 32 condensations observed toward this region is in good agreement with the hypothesis that the region is expanding with an expansion velocity smaller than 18 km s^{-1} .

6. In Corona Australis the velocity gradient changes from $-0.5 \text{ km s}^{-1} \text{ pc}^{-1}$ at one extreme to $+0.1 \text{ km s}^{-1} \text{ pc}^{-1}$ at the other. Among the nine filaments that comprise this cloud complex, there is star formation activity only

toward the CrA cloud, where five condensations were selected, and the filament C.

7. The clouds in Corona Australis, and Lupus and the condensations in the Scorpius region seem to be associated with expanding shells of gas and dust produced by the Upper Centaurus–Lupus and Upper Scorpius associations.

J. W. S. V. B. acknowledges the support of the Fundação de Amparo a Pesquisa do Estado de São Paulo (Brasil) Postdoctoral Fellowship and the Smithsonian Astrophysical Observatory for support of a Visiting Scientist Position. G. A. F. acknowledges a National Radio Astronomy Observatory Jansky Fellowship. The authors would like to thank the staff members of the SEST radio telescope, who made these observations possible. This research was (partially) supported by a grant from NASA administered by the American Astronomical Society.

REFERENCES

- Alvarez, H., Bronfman, R., Cohen, G., Garay, G., Graham, J., & Thaddeus, P. 1986, *ApJ*, 300, 756
- Andreazza, C., & Vilas-Boas, J. W. S. 1996, *A&AS*, 116, 21 (AV)
- Beichman, C. A., Neugebauer, G., Habing, H. J., Clegg, P. E., & Chester, T. J. 1984, *IRAS Catalog & Atlases, Explanatory Supplement* (Washington, DC: US GPO)
- Blaauw, A. 1964, *ARA&A*, 2, 213
- Bohlin, R. C., Savage, B. D., & Drake, J. F. 1978, *ApJ*, 224, 132
- Burton, W. B., & Litz, H. S. 1983, *A&AS*, 52, 63
- Cappa de Nicolau, E. C., & Pöppel, W. G. L. 1986, *A&A*, 164, 274
- . 1991, *A&AS*, 88, 615
- Chen, H., Myers, P. C., Ladd, E. F., & Wood, D. O. S. 1995, *ApJ*, 445, 377
- Cohen, M., & Schwartz, R. D. 1984, *AJ*, 89, 277
- Cumbrésy, L. 1999, *A&A*, 345, 965
- de Geus, E. 1988, Ph.D. thesis, Univ. Leiden
- de Geus, E. J. 1992, *A&A*, 262, 258
- Forveille, T., Guilloteau, S., & Lucas, R. 1989, *Software Package for Deducing Continuum and Spectroscopic Data* (Grenoble: Obs. Grenoble)
- Frerking, M. A., Langer, W. D., & Wilson, R. L. 1982, *ApJ*, 232, L89
- Gahm, G. F., Johansson, L. E. B., & Liseau, R. 1993, *A&A*, 274, 415
- Gauvin, L. S., & Strom, K. M. 1992, *ApJ*, 385, 217
- Goss, W. M., Manchester, R. N., Brooks, J. W., Sinclair, M. W., & Manfield, G. A. 1980, *MNRAS*, 191, 533
- Graham, J. A. 1992, in *Low-Mass Star Formation in Southern Molecular Clouds*, ed. B. Reipurth (ESO Sci. Rep. 11; Garching: ESO), 185
- Graham, J. A., & Frogel, J. A. 1985, *ApJ*, 289, 331
- Gredel, R., van Dishoeck, E. F., & Black, J. H. 1994, *A&A*, 285, 300
- Harju, J., Haikala, L. K., Mattila, K., Mauersberger, R., Booth, R. S., & Nordh, H. J. 1993, *A&A*, 278, 569
- Hartley, M., Manchester, R. N., Smith, R. M., Tritton, S. B., & Goss, W. M. 1986, *A&AS*, 63, 27
- Herbig, G. H., & Bell, K. R. 1988, *Lick Obs. Bull.* 1111
- Hetem, J. C. G., Sanzovo, G. C., & Lepine, J. R. D. 1988, *A&AS*, 76, 347
- Heyer, M. H., & Graham, J. A. 1989, *PASP*, 100, 816
- Hughes, J., & Hartigan, P. 1993, *AJ*, 105, 571
- Krautter, J. 1991, in *Low-Mass Star Formation in Southern Molecular Clouds*, ed. B. Reipurth (ESO Sci. Rep. 11; Garching: ESO), 127
- Loren, B. R. 1979, *ApJ*, 227, 832
- Loren, B. R., & Wootten, H. A. 1986, *ApJ*, 306, 142
- Lynds, B. T. 1962, *ApJS*, 7, 1
- Motte, F., André, P., & Neri, R. 1998, *A&A*, 336, 150
- Murphy, D. C., Cohen, R., & May, J. 1986, *A&A*, 167, 234
- Myers, P. C., Linke, R., & Benson, P. J. 1983, *ApJ*, 264, 517 (MLB)
- Persi, P., Ferrari-Toniolo, M., Busso, M., Origlia, L., Robberto, M., Scaltriti, F., & Silvestro, G. 1990, *AJ*, 99, 303
- Reipurth, B. 1983, *A&A*, 117, 183
- Reipurth, B., & Graham, J. A. 1988, *A&A*, 202, 219
- Rossano, G. S. 1978, *AJ*, 83, 234
- Sahu, M. S. 1992, Ph.D. thesis, Univ. Groningen
- Sandqvist, A. 1977, *A&A*, 57, 467
- Sandqvist, A., & Lindros, K. P. 1976, *A&A*, 53, 179
- Schober, J. 1976, *A&A*, 25, 507
- Schwartz, R. D. 1977, *ApJS*, 35, 161
- Strom, S. E., Grasdalen, G. L., & Strom, K. M. 1974, *ApJ*, 191, 111
- Tachihara, K., Dobashi, K., Mizuno, A., Ogawa, H., & Fukui, Y. 1996, *PASJ*, 48, 489
- Taylor, K. N. R., & Storey, J. W. V. 1984, *MNRAS*, 209, 5P
- Turner, B. E., Rickard, L. J., & Xu, L. 1989, *ApJ*, 391, 158
- Vilas-Boas, J. W. S., Myers, P. C., & Fuller, G. A. 1994, *ApJ*, 433, 96 (VMF)
- Vrba, F. J. 1977, *AJ*, 92, 198
- Weaver, H. 1978, in *IAU Symp. 84, The Large-Scale Characteristics of the Galaxy*, ed. W. B. Burton (Dordrecht: Reidel), 295
- Weintraub, D. A. 1990, *ApJS*, 74, 575
- Whittet, D. C. B., Prust, T., & Wesselius, P. R. 1991, *MNRAS*, 249, 319
- Wilking, B. A., Greene, T. P., Lada, C. J., Meyer, M. R., & Young, E. T. 1992, *ApJ*, 397, 520
- Zealey, W. J., Ninkov, Z., Rice, E., Hartley, M., & Tritton, S. B. 1983, *Astrophys. Lett.*, 23, 774